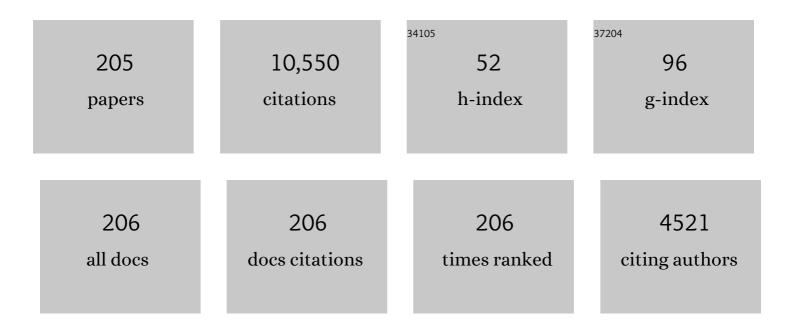
List of Publications by Year in descending order

Source: https://exaly.com/author-pdf/3780914/publications.pdf Version: 2024-02-01



#	Article	lF	CITATIONS
1	Characterization of Jason-3 Spacecraft Surface Charging in LEO Polar Regions From AMBER Observations. IEEE Transactions on Plasma Science, 2022, 50, 965-975.	1.3	1
2	Longâ€Term Variations of Quasiâ€Trapped and Trapped Electrons in the Inner Radiation Belt Observed by DEMETER and SAMPEX. Journal of Geophysical Research: Space Physics, 2020, 125, e2020JA028086.	2.4	4
3	The Dayâ€Night Difference and Geomagnetic Activity Variation of Energetic Electron Fluxes in Region of South Atlantic Anomaly. Space Weather, 2020, 18, e2020SW002479.	3.7	5
4	On the Ubiquity of Magnetic Reconnection Inside Flux Transfer Eventâ€Like Structures at the Earth's Magnetopause. Geophysical Research Letters, 2020, 47, e2019GL086726.	4.0	20
5	Latitudinal Dependence of the Kelvinâ€Helmholtz Instability and Beta Dependence of Vortexâ€Induced Highâ€Guide Field Magnetic Reconnection. Journal of Geophysical Research: Space Physics, 2020, 125, e2019JA027333.	2.4	7
6	Magnetic Reconnection Inside a Flux Transfer Eventâ€Like Structure in Magnetopause Kelvinâ€Helmholtz Waves. Journal of Geophysical Research: Space Physics, 2020, 125, e2019JA027527.	2.4	10
7	Precipitation of MeV and Subâ€MeV Electrons Due to Combined Effects of EMIC and ULF Waves. Journal of Geophysical Research: Space Physics, 2019, 124, 7923-7935.	2.4	17
8	AMBRE: A Compact Instrument to Measure Thermal Ions, Electrons and Electrostatic Charging Onboard Spacecraft. , 2019, , .		1
9	Four‣pacecraft Measurements of the Shape and Dimensionality of Magnetic Structures in the Near‣arth Plasma Environment. Journal of Geophysical Research: Space Physics, 2019, 124, 6850-6868.	2.4	7
10	Energetic Electrons Below the Inner Radiation Belt. Journal of Geophysical Research: Space Physics, 2019, 124, 5421-5440.	2.4	15
11	Cosmic Ray Albedo Neutron Decay (CRAND) as a Source of Inner Belt Electrons: Energy Spectrum Study. Geophysical Research Letters, 2019, 46, 544-552.	4.0	25
12	Lowâ€Altitude Observations of Recurrent Shortâ€Lived keV Ion Microinjections Inside the Diffuse Auroral Zone. Journal of Geophysical Research: Space Physics, 2018, 123, 2054-2063.	2.4	2
13	Magnetic Reconnection at a Thin Current Sheet Separating Two Interlaced Flux Tubes at the Earth's Magnetopause. Journal of Geophysical Research: Space Physics, 2018, 123, 1779-1793.	2.4	35
14	The Martian Photoelectron Boundary as Seen by MAVEN. Journal of Geophysical Research: Space Physics, 2017, 122, 10,472.	2.4	28
15	Comparative study of the Martian suprathermal electron depletions based on Mars Global Surveyor, Mars Express, and Mars Atmosphere and Volatile EvolutioN mission observations. Journal of Geophysical Research: Space Physics, 2017, 122, 857-873.	2.4	28
16	Electric Mars: A large transâ€ŧerminator electric potential drop on closed magnetic field lines above Utopia Planitia. Journal of Geophysical Research: Space Physics, 2017, 122, 2260-2271.	2.4	16
17	TARANIS XGRE and IDEE detection capability of terrestrial gamma-ray flashes and associated electron beams. Geoscientific Instrumentation, Methods and Data Systems, 2017, 6, 239-256.	1.6	10
18	A statistical study over Europe of the relative locations of lightning and associated energetic burst of electrons from the radiation belt. Annales Geophysicae, 2016, 34, 157-164.	1.6	5

#	Article	IF	CITATIONS
19	Currents and associated electron scattering and bouncing near the diffusion region at Earth's magnetopause. Geophysical Research Letters, 2016, 43, 3042-3050.	4.0	81
20	Fast Plasma Investigation for Magnetospheric Multiscale. Space Science Reviews, 2016, 199, 331-406.	8.1	960
21	Electron dynamics in a subprotonâ€gyroscale magnetic hole. Geophysical Research Letters, 2016, 43, 4112-4118.	4.0	49
22	Thick escaping magnetospheric ion layer in magnetopause reconnection with MMS observations. Geophysical Research Letters, 2016, 43, 6028-6035.	4.0	1
23	Signatures of complex magnetic topologies from multiple reconnection sites induced by Kelvinâ€Helmholtz instability. Journal of Geophysical Research: Space Physics, 2016, 121, 9926-9939.	2.4	35
24	Shift of the magnetopause reconnection line to the winter hemisphere under southward IMF conditions: Geotail and MMS observations. Geophysical Research Letters, 2016, 43, 5581-5588.	4.0	17
25	The MAVEN Solar Wind Electron Analyzer. Space Science Reviews, 2016, 200, 495-528.	8.1	217
26	Three-dimensional current systems and ionospheric effects associated with small dipolarization fronts. Journal of Geophysical Research: Space Physics, 2015, 120, 3739-3757.	2.4	16
27	Statistical study of magnetic cloud erosion by magnetic reconnection. Journal of Geophysical Research: Space Physics, 2015, 120, 43-60.	2.4	106
28	Altitude dependence of nightside Martian suprathermal electron depletions as revealed by MAVEN observations. Geophysical Research Letters, 2015, 42, 8877-8884.	4.0	41
29	Oxygen foreshock of Mars. Planetary and Space Science, 2015, 119, 48-53.	1.7	9
30	Seasonal variation of Martian pick-up ions: Evidence of breathing exosphere. Planetary and Space Science, 2015, 119, 54-61.	1.7	56
31	Electric Mars: The first direct measurement of an upper limit for the Martian "polar wind―electric potential. Geophysical Research Letters, 2015, 42, 9128-9134.	4.0	38
32	A hot flow anomaly at Mars. Geophysical Research Letters, 2015, 42, 9121-9127.	4.0	20
33	Birth of a comet magnetosphere: A spring of water ions. Science, 2015, 347, aaa0571.	12.6	107
34	Unexpected Very Low Frequency (VLF) Radio Events Recorded by the Ionospheric Satellite DEMETER. Surveys in Geophysics, 2015, 36, 483-511.	4.6	15
35	The Mars Atmosphere and Volatile Evolution (MAVEN) Mission. Space Science Reviews, 2015, 195, 3-48.	8.1	563
36	MAVEN observations of the response of Mars to an interplanetary coronal mass ejection. Science, 2015, 350, aad0210.	12.6	166

#	Article	IF	CITATIONS
37	Early MAVEN Deep Dip campaign reveals thermosphere and ionosphere variability. Science, 2015, 350, aad0459.	12.6	90
38	Solar windâ€driven thermospheric winds over the Venus North Polar region. Geophysical Research Letters, 2014, 41, 4413-4419.	4.0	4
39	Solar wind control of the terrestrial magnetotail as seen by STEREO. Journal of Geophysical Research: Space Physics, 2014, 119, 6342-6355.	2.4	10
40	Comment on "Comparative study on earthquake and ground based transmitter induced radiation belt electron precipitation at middle latitude", by Sideropoulos et al. (2011). Natural Hazards and Earth System Sciences, 2014, 14, 1-9.	3.6	12
41	Ninety degrees pitch angle enhancements of suprathermal electrons associated with interplanetary shocks. Journal of Geophysical Research: Space Physics, 2014, 119, 7038-7060.	2.4	7
42	A statistical analysis of properties of small transients in the solar wind 2007–2009: STEREO and Wind observations. Journal of Geophysical Research: Space Physics, 2014, 119, 689-708.	2.4	51
43	THEMIS observations of the current sheet dynamics in response to the intrusion of the highâ€velocity plasma flow into the nearâ€Earth magnetotail. Journal of Geophysical Research: Space Physics, 2014, 119, 6553-6568.	2.4	14
44	The effects and correction of the geometric factor for the POES/MEPED electron flux instrument using a multisatellite comparison. Journal of Geophysical Research: Space Physics, 2014, 119, 6386-6404.	2.4	17
45	Testing linear theory of EMIC waves in the inner magnetosphere: Cluster observations. Journal of Geophysical Research: Space Physics, 2014, 119, 1004-1027.	2.4	26
46	Inner radiation belt particle acceleration and energy structuring by drift resonance with ULF waves during geomagnetic storms. Journal of Geophysical Research: Space Physics, 2013, 118, 1723-1736.	2.4	48
47	Ionospheric density perturbations recorded by DEMETER above intense thunderstorms. Journal of Geophysical Research: Space Physics, 2013, 118, 5169-5176.	2.4	15
48	Energetic Charged Particles Above Thunderclouds. Surveys in Geophysics, 2013, 34, 1-41.	4.6	26
49	Current sheet structure and kinetic properties of plasma flows during a nearâ€Earth magnetic reconnection under the presence of a guide field. Journal of Geophysical Research: Space Physics, 2013, 118, 3265-3287.	2.4	29
50	Cluster observations of whistler waves correlated with ionâ€scale magnetic structures during the 17 August 2003 substorm event. Journal of Geophysical Research: Space Physics, 2013, 118, 6072-6089.	2.4	20
51	Statistical study of foreshock cavitons. Annales Geophysicae, 2013, 31, 2163-2178.	1.6	29
52	Solar windâ€driven plasma fluxes from the Venus ionosphere. Journal of Geophysical Research: Space Physics, 2013, 118, 7497-7506.	2.4	6
53	Determining the spectra of radiation belt electron losses: Fitting DEMETER electron flux observations for typical and storm times. Journal of Geophysical Research: Space Physics, 2013, 118, 7611-7623.	2.4	41
54	A largeâ€scale flow vortex in the Venus plasma tail and its fluid dynamic interpretation. Geophysical Research Letters, 2013, 40, 1273-1278.	4.0	16

#	Article	IF	CITATIONS
55	On the problem of Plasma Sheet Boundary Layer identification from plasma moments in Earth's magnetotail. Annales Geophysicae, 2012, 30, 1331-1343.	1.6	12
56	Ion acceleration by multiple reflections at Martian bow shock. Earth, Planets and Space, 2012, 64, 61-71.	2.5	6
57	Coupling Between Whistler Waves and Ion-Scale Solitary Waves: Cluster Measurements in the Magnetotail During a Substorm. Physical Review Letters, 2012, 109, 155005.	7.8	12
58	The Heliospheric Plasma Sheet Observed in situ by Three Spacecraft over Four Solar Rotations. Solar Physics, 2012, 281, 423.	2.5	19
59	THE SOLAR ORIGIN OF SMALL INTERPLANETARY TRANSIENTS. Astrophysical Journal, 2011, 734, 7.	4.5	89
60	PLASMOID RELEASES IN THE HELIOSPHERIC CURRENT SHEET AND ASSOCIATED CORONAL HOLE BOUNDARY LAYER EVOLUTION. Astrophysical Journal, 2011, 737, 16.	4.5	32
61	Ion flow and momentum transfer in the Venus plasma environment. Icarus, 2011, 215, 751-758.	2.5	46
62	The IMPACT Solar Wind Electron Analyzer (SWEA): Reconstruction of the SWEA Transmission Function by Numerical Simulation and Data Analysis. Space Science Reviews, 2011, 161, 49-62.	8.1	11
63	Non-adiabatic Ion Acceleration in the Earth Magnetotail and Its Various Manifestations in the Plasma Sheet Boundary Layer. Space Science Reviews, 2011, 164, 133-181.	8.1	33
64	Comparison of accelerated ion populations observed upstream of the bow shocks at Venus and Mars. Annales Geophysicae, 2011, 29, 511-528.	1.6	22
65	Solar-Wind Bulk Velocity Throughout the Inner Heliosphere from Multi-Spacecraft Measurements. Solar Physics, 2010, 264, 377-382.	2.5	17
66	Temporal Evolution of the Solar-Wind Electron Core Density at Solar Minimum by Correlating SWEA Measurements from STEREO A and B. Solar Physics, 2010, 266, 369-377.	2.5	5
67	The Mercury Electron Analyzers for the Bepi Colombo mission. Advances in Space Research, 2010, 46, 1139-1148.	2.6	14
68	Statistics of counter-streaming solar wind suprathermal electrons at solar minimum: STEREO observations. Annales Geophysicae, 2010, 28, 233-246.	1.6	24
69	Large-scale fluctuations of PSBL magnetic flux tubes induced by the field-aligned motion of highly accelerated ions. Annales Geophysicae, 2010, 28, 1273-1288.	1.6	15
70	Cross-scale: multi-scale coupling in space plasmas. Experimental Astronomy, 2009, 23, 1001-1015.	3.7	18
71	Multispacecraft Observations of Magnetic Clouds andÂTheir Solar Origins between 19 and 23 May 2007. Solar Physics, 2009, 254, 325-344.	2.5	68
72	A Multispacecraft Analysis of a Small-Scale Transient Entrained by Solar Wind Streams. Solar Physics, 2009, 256, 307-326.	2.5	93

#	Article	IF	CITATIONS
73	Observation of a Complex Solar Wind Reconnection Exhaust from Spacecraft Separated by over 1800 R E. Solar Physics, 2009, 256, 379-392.	2.5	39
74	On the Temporal Variability of the "Strahl―andÂltsÂRelationship with Solar Wind Characteristics: STEREO SWEA Observations. Solar Physics, 2009, 259, 311-321.	2.5	9
75	The Apparent Layered Structure of the Heliospheric Current Sheet: Multi-Spacecraft Observations. Solar Physics, 2009, 259, 389-416.	2.5	28
76	Signatures of interchange reconnection: STEREO, ACE and Hinode observations combined. Annales Geophysicae, 2009, 27, 3883-3897.	1.6	29
77	TARANIS—A Satellite Project Dedicated to the Physics of TLEs and TGFs. Space Science Reviews, 2008, 137, 301-315.	8.1	41
78	Location of the bow shock and ion composition boundaries at Venus—initial determinations from Venus Express ASPERA-4. Planetary and Space Science, 2008, 56, 780-784.	1.7	64
79	The Venusian induced magnetosphere: A case study of plasma and magnetic field measurements on the Venus Express mission. Planetary and Space Science, 2008, 56, 796-801.	1.7	22
80	Mars Express and Venus Express multi-point observations of geoeffective solar flare events in December 2006. Planetary and Space Science, 2008, 56, 873-880.	1.7	102
81	The magnetic field near Mars: A comparison between a hybrid model, Mars Global Surveyor and Mars Express observations. Planetary and Space Science, 2008, 56, 828-831.	1.7	0
82	Ionospheric photoelectrons at Venus: Initial observations by ASPERA-4 ELS. Planetary and Space Science, 2008, 56, 802-806.	1.7	48
83	Advanced method to derive the IMF direction near Mars from cycloidal proton distributions. Planetary and Space Science, 2008, 56, 1145-1154.	1.7	10
84	Radiation belt electron precipitation due to VLF transmitters: Satellite observations. Geophysical Research Letters, 2008, 35, .	4.0	105
85	Radiation belt electron precipitation by manâ€made VLF transmissions. Journal of Geophysical Research, 2008, 113, .	3.3	73
86	Transient and localized processes in the magnetotail: a review. Annales Geophysicae, 2008, 26, 955-1006.	1.6	112
87	An assessment of the role of the centrifugal acceleration mechanism in high altitude polar cap oxygen ion outflow. Annales Geophysicae, 2008, 26, 145-157.	1.6	38
88	Conjugate observation of sharp dynamical boundary in the inner magnetosphere by Cluster and DMSP spacecraft and ground network. Annales Geophysicae, 2008, 26, 2771-2780.	1.6	5
89	Transients in oxygen outflow above the polar cap as observed by the Cluster spacecraft. Annales Geophysicae, 2008, 26, 3365-3373.	1.6	19
90	A case study of dayside reconnection under extremely low solar wind density conditions. Annales Geophysicae, 2008, 26, 3571-3583.	1.6	1

#	Article	IF	CITATIONS
91	Multi-spacecraft observation of plasma dipolarization/injection in the inner magnetosphere. Annales Geophysicae, 2007, 25, 801-814.	1.6	88
92	Martian Atmospheric Erosion Rates. Science, 2007, 315, 501-503.	12.6	248
93	Ion multi-nose structures observed by Cluster in the inner Magnetosphere. Annales Geophysicae, 2007, 25, 171-190.	1.6	42
94	Dynamics of thin current sheets: Cluster observations. Annales Geophysicae, 2007, 25, 1365-1389.	1.6	83
95	CLUSTER observations of electron outflowing beams carrying downward currents above the polar cap by northward IMF. Annales Geophysicae, 2007, 25, 953-969.	1.6	17
96	The Analyser of Space Plasmas and Energetic Atoms (ASPERA-4) for the Venus Express mission. Planetary and Space Science, 2007, 55, 1772-1792.	1.7	214
97	Rosina – Rosetta Orbiter Spectrometer for Ion and Neutral Analysis. Space Science Reviews, 2007, 128, 745-801.	8.1	331
98	RPC-ICA: The Ion Composition Analyzer of the Rosetta Plasma Consortium. Space Science Reviews, 2007, 128, 671-695.	8.1	104
99	The Analyzer of Space Plasmas and Energetic Atoms (ASPERA-3) for the Mars Express Mission. Space Science Reviews, 2007, 126, 113-164.	8.1	241
100	Local structure of the magnetotail current sheet: 2001 Cluster observations. Annales Geophysicae, 2006, 24, 247-262.	1.6	220
101	Observation of mixed ion populations deep inside earth magnetosphere as evidence for reconnection during northward IMF with substantial By component. Advances in Space Research, 2006, 37, 1394-1401.	2.6	1
102	Imprints of non-adiabatic ion acceleration in the earth's magnetotail: Interball observations and statistical analysis. Advances in Space Research, 2006, 38, 37-46.	2.6	0
103	Electric fields within the martian magnetosphere and ion extraction: ASPERA-3 observations. Icarus, 2006, 182, 337-342.	2.5	54
104	Solar wind plasma protrusion into the martian magnetosphere: ASPERA-3 observations. Icarus, 2006, 182, 343-349.	2.5	21
105	First ENA observations at Mars: Subsolar ENA jet. Icarus, 2006, 182, 413-423.	2.5	42
106	First ENA observations at Mars: ENA emissions from the martian upper atmosphere. Icarus, 2006, 182, 424-430.	2.5	53
107	Structure of the martian wake. Icarus, 2006, 182, 329-336.	2.5	81
108	First ENA observations at Mars: Charge exchange ENAs produced in the magnetosheath. Icarus, 2006, 182. 431-438.	2.5	39

#	Article	IF	CITATIONS
109	Electron oscillations in the induced martian magnetosphere. Icarus, 2006, 182, 360-370.	2.5	54
110	Observations of magnetic anomaly signatures in Mars Express ASPERA-3 ELS data. Icarus, 2006, 182, 396-405.	2.5	36
111	Ionospheric plasma acceleration at Mars: ASPERA-3 results. Icarus, 2006, 182, 308-319.	2.5	48
112	Numerical interpretation of high-altitude photoelectron observations. Icarus, 2006, 182, 383-395.	2.5	56
113	Plasma intrusion above Mars crustal fields—Mars Express ASPERA-3 observations. Icarus, 2006, 182, 406-412.	2.5	35
114	Energetic Neutral Atoms (ENA) at Mars: Properties of the hydrogen atoms produced upstream of the martian bow shock and implications for ENA sounding technique around non-magnetized planets. Icarus, 2006, 182, 448-463.	2.5	22
115	First ENA observations at Mars: Solar-wind ENAs on the nightside. Icarus, 2006, 182, 439-447.	2.5	27
116	Carbon dioxide photoelectron energy peaks at Mars. Icarus, 2006, 182, 371-382.	2.5	105
117	Ion escape at Mars: Comparison of a 3-D hybrid simulation with Mars Express IMA/ASPERA-3 measurements. Icarus, 2006, 182, 350-359.	2.5	34
118	Mass composition of the escaping plasma at Mars. Icarus, 2006, 182, 320-328.	2.5	103
119	Plasma Acceleration Above Martian Magnetic Anomalies. Science, 2006, 311, 980-983.	12.6	111
120	Characteristics of high altitude oxygen ion energization and outflow as observed by Cluster: a statistical study. Annales Geophysicae, 2006, 24, 1099-1112.	1.6	55
121	A multi-satellite study of accelerated ionospheric ion beams above the polar cap. Annales Geophysicae, 2006, 24, 1665-1684.	1.6	27
122	Accelerated electrons in the LLBL as observed by Interball on February 15, 1996. Planetary and Space Science, 2005, 53, 149-156.	1.7	0
123	Statistical studies of geomagnetic storm dependencies on solar and interplanetary events: a review. Planetary and Space Science, 2005, 53, 189-196.	1.7	76
124	Bifurcated current sheet: model and Cluster observations. Planetary and Space Science, 2005, 53, 229-235.	1.7	25
125	Spatial structure of beamlets according to Cluster observations. Planetary and Space Science, 2005, 53, 245-254.	1.7	4
126	Magnetosheath Interaction with the High Latitude Magnetopause. Surveys in Geophysics, 2005, 26, 95-133.	4.6	23

#	Article	IF	CITATIONS
127	Spatial and Temporal Cusp Structures Observed by Multiple Spacecraft and Ground Based Observations. Surveys in Geophysics, 2005, 26, 281-305.	4.6	10
128	Formation of the flank LLBL: A case study. European Physical Journal D, 2005, 55, 1293-1301.	0.4	0
129	Electric current and magnetic field geometry in flapping magnetotail current sheets. Annales Geophysicae, 2005, 23, 1391-1403.	1.6	171
130	Survey of energetic O ⁺ ions near the dayside mid-latitude magnetopause with Cluster. Annales Geophysicae, 2005, 23, 1281-1294.	1.6	27
131	Magnetospheric plasma boundaries: a test of the frozen-in magnetic field theorem. Annales Geophysicae, 2005, 23, 2565-2578.	1.6	6
132	Transition from substorm growth to substorm expansion phase as observed with a radial configuration of ISTP and Cluster spacecraft. Annales Geophysicae, 2005, 23, 2183-2198.	1.6	33
133	Energetic particle injections into the outer cusp during compression events. Earth, Planets and Space, 2005, 57, 125-130.	2.5	4
134	The HIA instrument on board the Tan Ce 1 Double Star near-equatorial spacecraft and its first results. Annales Geophysicae, 2005, 23, 2757-2774.	1.6	76
135	The structure of high altitude O ⁺ energization and outflow: a case study. Annales Geophysicae, 2004, 22, 2497-2506.	1.6	33
136	Evidence for storm-time ionospheric ion precipitation in the cusp with magnetosheath energy. Annales Geophysicae, 2004, 22, 1765-1771.	1.6	1
137	On the altitude dependence of transversely heated O ⁺ distributions in the cusp/cleft. Annales Geophysicae, 2004, 22, 1787-1798.	1.6	62
138	The exterior cusp and its boundary with the magnetosheath: Cluster multi-event analysis. Annales Geophysicae, 2004, 22, 3039-3054.	1.6	47
139	Multipoint analysis of the spatio-temporal coherence of dayside O ⁺ outflows with Cluster. Annales Geophysicae, 2004, 22, 2507-2514.	1.6	14
140	Bow shock specularly reflected ions in the presence of low-frequency electromagnetic waves: a case study. Annales Geophysicae, 2004, 22, 2325-2335.	1.6	34
141	Solar Wind-Induced Atmospheric Erosion at Mars: First Results from ASPERA-3 on Mars Express. Science, 2004, 305, 1933-1936.	12.6	204
142	A low-power timing discriminator for space instrumentation. Review of Scientific Instruments, 2004, 75, 5100-5105.	1.3	0
143	DYNAMO: a Mars upper atmosphere package for investigating solar wind interaction and escape processes, and mapping Martian fields. Advances in Space Research, 2004, 33, 2228-2235.	2.6	3
144	Cluster observations of complex 3D magnetic structures at the magnetopause. Geophysical Research Letters, 2004, 31, .	4.0	24

#	Article	IF	CITATIONS
145	Pulsed flows at the high-altitude cusp poleward boundary, and associated ionospheric convection and particle signatures, during a Cluster - FAST - SuperDARN- SÃ,ndrestrÃ,m conjunction under a southwest IMF. Annales Geophysicae, 2004, 22, 2891-2905.	1.6	23
146	Magnetosheath-cusp interface. Annales Geophysicae, 2004, 22, 183-212.	1.6	35
147	Title is missing!. Cosmic Research, 2003, 41, 3-12.	0.6	24
148	Fine structure of the polar cusp as deduced from the plasma wave and plasma measurements. Advances in Space Research, 2003, 32, 315-321.	2.6	6
149	Coupling of transient plasma structures observed in the plasma sheet boundary layer and in the auroral region. Advances in Space Research, 2003, 31, 1271-1276.	2.6	4
150	Evidence for impulsive solar wind plasma penetration through the dayside magnetopause. Annales Geophysicae, 2003, 21, 457-472.	1.6	51
151	Observation of energy-time dispersed ion structures in the magnetosheath by CLUSTER: possible signatures of transient acceleration processes at shock. Annales Geophysicae, 2003, 21, 1483-1495.	1.6	10
152	Modeling transverse heating and outflow of ionospheric ions from the dayside cusp/cleft. 2 Applications. Annales Geophysicae, 2003, 21, 1773-1791.	1.6	29
153	Cusp structures: combining multi-spacecraft observations with ground-based observations. Annales Geophysicae, 2003, 21, 2031-2041.	1.6	20
154	Equator-S observations of He+energization by EMIC waves in the dawnside equatorial magnetosphere. Geophysical Research Letters, 2002, 29, 74-1-74-4.	4.0	23
155	<i>Introduction</i> The Interball project after 6 years of data analysis. Annales Geophysicae, 2002, 20, 289-291.	1.6	0
156	Plasma sheet fast flows and auroral dynamics during substorm: a case study. Annales Geophysicae, 2002, 20, 341-347.	1.6	7
157	Two types of ion spectral gaps in the quiet inner magnetosphere: Interball-2 observations and modeling. Annales Geophysicae, 2002, 20, 349-364.	1.6	28
158	Density profile in the magnetosheath adjacent to the magnetopause. Advances in Space Research, 2002, 30, 1693-1703.	2.6	6
159	Accelerated particles from turbulent boundary layer. Advances in Space Research, 2002, 30, 1723-1730.	2.6	9
160	The electron mixing and acceleration signatures as seen near the cusp and on the flank. Advances in Space Research, 2002, 30, 1731-1740.	2.6	0
161	Auroral signatures of transient processes in the outer magnetosphere. Advances in Space Research, 2002, 30, 2701-2711.	2.6	3
162	On the origin of the high-latitude boundary layer. Advances in Space Research, 2002, 30, 2763-2770.	2.6	6

#	Article	IF	CITATIONS
163	Interconnection of high-latitude and low-latitude boundary layers when IMF BY is dominant. Advances in Space Research, 2002, 30, 2771-2779.	2.6	1
164	Mid-latitude reflection of ion upflows during substorm dipolarization. Geophysical Research Letters, 2001, 28, 475-478.	4.0	0
165	A study of ion injections at the dawn and dusk polar edges of the auroral oval. Journal of Geophysical Research, 2001, 106, 29619-29631.	3.3	20
166	Scientific objectives of the DYNAMO mission. Advances in Space Research, 2001, 27, 1851-1860.	2.6	4
167	Correlated Interball/ground-based observations of isolated substorm: The pseudobreakup phase. Annales Geophysicae, 2001, 19, 687-698.	1.6	13
168	A physical 4D radiation belt model including a time dependent magnetic field. Advances in Space Research, 2000, 25, 2303-2306.	2.6	2
169	Plasma characteristics of high-altitude cusp for steady southward-dawnward IMF. Advances in Space Research, 2000, 25, 1435-1444.	2.6	1
170	Multi-spacecraft observations of series of substorms on December 22–23, 1996. Advances in Space Research, 2000, 25, 1697-1701.	2.6	0
171	Coordinated Wind, Interball/tail, and ground observations of Kelvin-Helmholtz waves at the near-tail, equatorial magnetopause at dusk: January 11, 1997. Journal of Geophysical Research, 2000, 105, 7639-7667.	3.3	53
172	Plasma sheet ion injections into the auroral bulge: Correlative study of spacecraft and ground observations. Journal of Geophysical Research, 2000, 105, 18465-18481.	3.3	37
173	Magnetopause boundary structure deduced from the high-time resolution particle experiment on the Equator-S spacecraft. Annales Geophysicae, 1999, 17, 1574-1581.	1.6	1
174	Testing electric field models using ring current ion energy spectra from the Equator-S ion composition (ESIC) instrument. Annales Geophysicae, 1999, 17, 1611-1621.	1.6	39
175	Venus-like interaction of the solar wind with Mars. Geophysical Research Letters, 1999, 26, 2685-2688.	4.0	114
176	Sporadic plasma sheet ion injections into the high-altitude auroral bulge: Satellite observations. Journal of Geophysical Research, 1999, 104, 28565-28586.	3.3	53
177	On the origin of sporadic keV ion injections observed by Interball-Auroral during the expansion phase of a substorm. Journal of Geophysical Research, 1999, 104, 24929-24937.	3.3	9
178	INTERBALL-Auroral observations of 0.1-12 keV ion gaps in the diffuse auroral zone. Annales Geophysicae, 1999, 17, 734.	1.6	7
179	The ion experiment onboard the Interball-Aurora satellite; initial results on velocity-dispersed structures in the cleft and inside the auroral oval. Annales Geophysicae, 1998, 16, 1056-1069.	1.6	47
180	Magnetic Field and Plasma Observations at Mars: Initial Results of the Mars Global Surveyor Mission. Science, 1998, 279, 1676-1680.	12.6	670

#	Article	IF	CITATIONS
181	Gross deformation of the dayside magnetopause. Geophysical Research Letters, 1998, 25, 453-456.	4.0	53
182	The INTERBALL-Tail ELECTRON experiment: initial results on the low-latitude boundary layer of the dawn magnetosphere. Annales Geophysicae, 1997, 15, 587-595.	1.6	72
183	Two-point measurement of hot plasma structures in the magnetotail lobes. Advances in Space Research, 1997, 20, 993-997.	2.6	6
184	Cusp and boundary layer observations by INTERBALL. Advances in Space Research, 1997, 20, 823-832.	2.6	21
185	Special Topic. Annales Geophysicae, 1997, 15, 511.	1.6	0
186	Signatures of impulsive convection in the magnetospheric lobes. Geophysical Research Letters, 1996, 23, 129-132.	4.0	13
187	Large Scale Dynamics of the Magnetospheric Tail Induced by Substorms: A Multisatellite Study. Journal of Geomagnetism and Geoelectricity, 1996, 48, 675-686.	0.9	7
188	Centrifugal trapping in the magnetotail. Annales Geophysicae, 1995, 13, 242-246.	1.6	5
189	Tailward propagating crossâ€tail current disruption and dynamics of nearâ€Earth Tail: A multiâ€point measurement analysis. Geophysical Research Letters, 1993, 20, 983-986.	4.0	99
190	Gyroâ€phase effects near the stormâ€time boundary of energetic plasma. Geophysical Research Letters, 1991, 18, 1485-1488.	4.0	11
191	Location and propagation of the magnetotail current disruption during substorm expansion: Analysis and simulation of an ISEE multiâ€onset event. Geophysical Research Letters, 1991, 18, 389-392.	4.0	173
192	Negative ions in the coma of comet Halley. Nature, 1991, 349, 393-396.	27.8	203
193	Dynamics of singleâ€particle orbits during substorm expansion phase. Journal of Geophysical Research, 1990, 95, 20853-20865.	3.3	135
194	Probable detection of organic-dust-borne aromatic C3H3+ ions in the coma of comet Halley. Nature, 1989, 337, 53-55.	27.8	51
195	Analysis of suprathermal electron properties at the magnetic pileâ€up boundary of comet P/Halley. Geophysical Research Letters, 1989, 16, 1035-1038.	4.0	47
196	Evidence for Chain Molecules Enriched in Carbon, Hydrogen, and Oxygen in Comet Halley. Science, 1987, 237, 626-628.	12.6	84
197	The heavy ion analyser PICCA for the Comet Halley fly-by with Giotto. Journal of Physics E: Scientific Instruments, 1987, 20, 787-792.	0.7	10
198	The Giotto electron plasma experiment. Journal of Physics E: Scientific Instruments, 1987, 20, 721-731.	0.7	11

#	Article	IF	CITATIONS
199	Giotto measurements of cometary and solar wind plasma at the Comet Halley bow shock. Nature, 1987, 327, 489-492.	27.8	28
200	Mass spectra of heavy ions near comet Halley. Nature, 1986, 321, 335-336.	27.8	61
201	Comet Halley–solar wind interaction from electron measurements aboard Giotto. Nature, 1986, 321, 349-352.	27.8	78
202	A multisatellite study of the plasma sheet dynamics at substorm onset. Geophysical Research Letters, 1984, 11, 500-503.	4.0	20
203	Drift boundaries and ULF wave generation near noon at geostationary orbit. Geophysical Research Letters, 1983, 10, 639-642.	4.0	15
204	A statistical study of the dynamics of the equatorward boundary of the diffuse aurora in the preâ€midnight sector. Geophysical Research Letters, 1983, 10, 749-752.	4.0	15
205	Morning sector ion precipitation following substorm injections. Journal of Geophysical Research, 1981. 86. 3430-3438.	3.3	33